

Identification of Spin Diffusion Pathways in Isotopically Labeled Biomolecules

Thomas R. Eykyn,* Dominique Früh,* and Geoffrey Bodenhausen*[†]

*Section de Chimie, Université de Lausanne, BCH, 1015 Lausanne, Switzerland; and [†]Département de chimie, associé au CNRS, Ecole Normale Supérieure, 24 rue Lhomond, 75231 Paris cedex 05, France

Received December 22, 1998

One-dimensional NOE experiments applicable to labeled macromolecules are presented which allow the manipulation of specific spin diffusion pathways and thus unambiguously identify clandestine spins through which the direct NOE is mediated. A treatment of spin diffusion using average Liouvillian theory is shown to describe adequately these phenomena. Experiments are carried out on an ¹⁵N-labeled sample of human ubiquitin. © 1999

Academic Press

Key Words: selective NOE; spin diffusion; average Liouvillian theory; protein NMR.

The observation of NOEs between noncontiguous structural units can yield knowledge about the global fold of proteins and about their tertiary solution-state structures (*I*). In the two-spin approximation the initial buildup of the NOE is proportional to r^{-6} , where r is the distance between source and target protons, provided the motion can be described by a single correlation time. However, one must exercise caution when calculating distances from NOEs since the flow of magnetization may be transferred via intermediate “clandestine” spins, thus introducing large errors into these measurements. Consequently a great deal of work has emerged within the past 10 years to remove the effects of spin diffusion and thus obtain more reliable distances (2–9). In general the flow of magnetization must be confined within subnetworks of the complete spin system, the ultimate goal being the complete removal of all spin diffusion contributions. However, the observation of an NOE between two protons, in the absence of further information, will only yield a distance constraint that positions the target proton somewhere on a sphere centered on the source proton. It would therefore be advantageous if one could not only distinguish the source and target spins but also the clandestine spins through which the indirect NOE is mediated. This can be achieved through a combination of single and triple inversion experiments, as will be shown below. This adds an additional degree of directionality to the NOE that may assist in conformational studies. A recent investigation (*10*) of amide–amide NOEs in a

¹⁵N-labeled protein has shown that one may selectively discriminate between spin diffusion pathways mediated via backbone CH or CH₂ groups. In this Communication we propose an adaptation of a recent 1D NOE experiment (*11*), applicable to isotopically labeled macromolecules, which allows the identification of a specific spin diffusion pathway within a protein. These effects are discussed within an average Liouvillian framework (*12–14*).

Consider an arbitrary system of three spins I_1 , I_2 , and I_3 , where I_1 is the source spin, I_3 the target, and I_2 an intermediate spin through which the NOE is mediated. The relaxation matrix for this three-spin subspace may be written as

$$\Gamma = \begin{bmatrix} \rho_1 & \sigma_{12} & \sigma_{13} \\ \sigma_{12} & \rho_2 & \sigma_{23} \\ \sigma_{13} & \sigma_{23} & \rho_3 \end{bmatrix}, \quad [1]$$

where ρ_i and σ_{ij} are the familiar auto- and cross-relaxation rate constants, respectively. We may then consider the effect of inverting spin I_2 at time $\tau_m/2$ in terms of average Liouvillian theory. The density operator at the end of the mixing time is given by

$$\sigma(\tau_m) = \exp\left(-\Gamma'_2 \frac{\tau_m}{2}\right) \exp\left(-\Gamma'_1 \frac{\tau_m}{2}\right) \sigma'(0), \quad [2]$$

where $\sigma'(0)$ is a transformed initial density matrix. If the inversion of the magnetization of I_2 in the middle of τ_m is described by a matrix U , we have

$$\Gamma'_2 = \Gamma$$

$$\Gamma'_1 = U\Gamma U^{-1} = \begin{bmatrix} \rho_1 & -\sigma_{12} & \sigma_{13} \\ -\sigma_{12} & \rho_2 & -\sigma_{23} \\ \sigma_{13} & -\sigma_{23} & \rho_3 \end{bmatrix}, \quad [3]$$

where

$$U = \begin{bmatrix} 1 & 0 & 0 \\ 0 & -1 & 0 \\ 0 & 0 & 1 \end{bmatrix}. \quad [4]$$

[†] To whom correspondence should be addressed. Geoffrey.Bodenhausen@ens.fr. Fax: +33 1 44 32 33 97.

The zero-order average Liouvillian is therefore given by

$$\Gamma^{(0)} = \frac{1}{2} [\Gamma'_2 + \Gamma'_1] = \begin{bmatrix} \rho_1 & 0 & \sigma_{13} \\ 0 & \rho_2 & 0 \\ \sigma_{13} & 0 & \rho_3 \end{bmatrix}. \quad [5]$$

It is evident that the cross-relaxation via spin I_2 has been eliminated to zero order. The average Liouvillian also contains higher order terms that describe imperfect suppression at longer mixing times. The first-order correction is given by

$$\Gamma^{(1)} = -\frac{1}{2\tau_m} \left[\Gamma'_1 \frac{\tau_m}{2}, \Gamma'_2 \frac{\tau_m}{2} \right]$$

$$\Gamma^{(1)} = \frac{\tau_m}{4} \begin{bmatrix} 0 & (\rho_1\sigma_{12} - \rho_2\sigma_{12} + \sigma_{13}\sigma_{23}) & 0 \\ (-\rho_1\sigma_{12} + \rho_2\sigma_{12} - \sigma_{13}\sigma_{23}) & 0 & (-\rho_3\sigma_{23} + \rho_2\sigma_{23} - \sigma_{12}\sigma_{13}) \\ 0 & (\rho_3\sigma_{23} - \rho_2\sigma_{23} + \sigma_{12}\sigma_{13}) & 0 \end{bmatrix}. \quad [6]$$

Figure 1 shows a comparison of an exact integration of the Solomon equations with a simulation using an average Liouvillian composed of zero- and first-order terms and a 3×3 relaxation matrix derived from experimental data. Simulations correspond to a single inversion of spin I_2 at $\tau_m/2$. The two approaches agree well for short mixing times, but diverge as higher order corrections to the average Liouvillian become necessary. Relaxation during the inversion pulse was neglected. It should be noted that in reality, for a nonideal pulse, the midpoint of the mixing time becomes ill-defined as the inversion is only really defined at the end of the pulse. The

situation is further complicated for pulses that exhibit complex trajectories of the magnetization (15).

The pulse sequences used in Fig. 2 are closely related to a recent selective NOE experiment (11). Selectivity is achieved using two-way cross-polarization to shuttle the magnetization from H^N to ^{15}N and back. This leads to a selective excitation of I_{1z} which may be considered to be essentially instantaneous, such that no cross-relaxation can occur during excitation. For normal NOE measurements two hard π pulses, which do not affect the relaxation behavior, were inserted during the mixing

time at $\tau_m/4$ and $3\tau_m/4$ to diminish the recovery of longitudinal components, notably of the water resonance. There is no need for further water suppression techniques. To investigate spin diffusion a selective π pulse is inserted at $\tau_m/2$ with the carrier positioned at the chemical shift of a chosen clandestine proton. This inverts the sign of the NOE between the source and the selected proton and therefore suppresses to zero order any two-step transfer that involves this selected proton. Application of selective pulses in such experiments leads to an increase of the water resonance. Convolution of the time domain data (16) was used to eliminate the water signal.

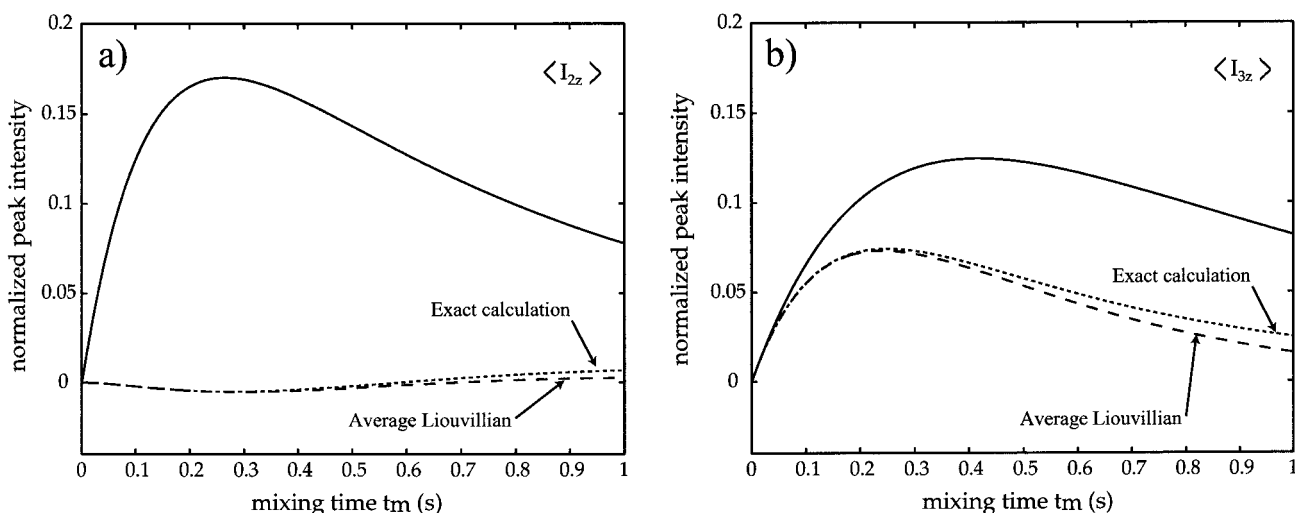


FIG. 1. Comparison of exact calculations with simulations using an average Liouvillian composed of zero- and first-order terms for the three-spin system defined in Eqs. [1–6]. (a) Buildup of I_{2z} without inversion (solid line) and remaining I_{2z} after its inversion (dashed and dotted lines). (b) Buildup of I_{3z} with and without inversion of I_{2z} .

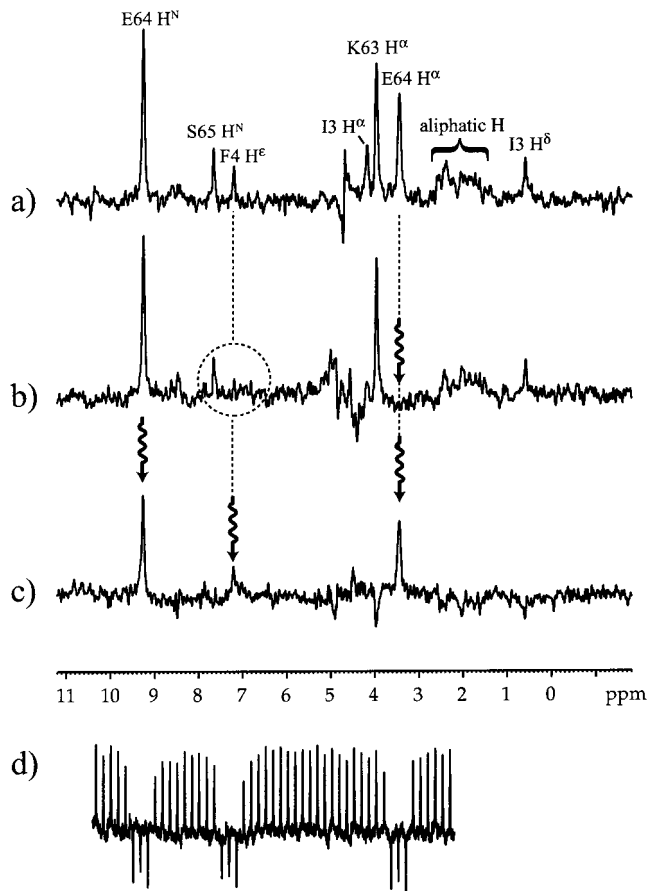


FIG. 2. (a) 1D NOE spectrum with a mixing time of 400 ms where the source proton is H^N in glutamic acid E64 of human ubiquitin, showing NOEs to various target protons. (b) Spectrum recorded with an I-Burp2 inversion pulse applied to H^α of E64. The $E64 H^\alpha$ and $F4 H^\epsilon$ resonances disappear. (c) Spectrum recorded with a triply modulated pulse for simultaneous inversion of spins H^N and H^α in E64, and H^ϵ in F4. The carrier frequency is positioned at the midpoint between resonances $E64 H^N$ and $E64 H^\alpha$. The $E64 H^\alpha$ and $F4 H^\epsilon$ resonances reappear. Overall the spectrum is attenuated with respect to (a) and (b) due to the triple inversion. All spectra are plotted to the same scale. Each spectrum took approximately 1 h with 2 k scans. (d) Inversion profile of $E64 H^N$ using a triply modulated I-Burp2 pulse.

All experiments were performed on a Bruker DRX 300 MHz spectrometer at 303 K with a 1.5 mM sample of ^{15}N -labeled human ubiquitin (VLI Research) in $H_2O:D_2O = 9:1$ buffered at $pH = 4.5$ with 20 mM perdeuterated acetic acid. The selective inversion pulse used in these experiments was a 40-ms I-Burp2 pulse (17) with a bandwidth of 120 Hz calibrated (18) for a proper inversion on-resonance.

Figure 2a shows a spectrum recorded for source proton $E64 H^N$ with a mixing time of 400 ms without quenching of spin diffusion. The spectrum shows the source proton and various target protons within its vicinity. Figure 2b displays the spectrum recorded using a selective inversion of $E64 H^\alpha$, resulting in almost complete suppression of its signal. One may also observe a substantial attenuation of $F4 H^\epsilon$ while the remaining NOEs remain largely unaffected. This is in agreement with an

NOE from $E64 H^N$ to $F4 H^\epsilon$ that is primarily mediated by a two-step transfer via $E64 H^\alpha$. Relaxation during the application of the selective pulse results in almost negligible attenuation of the noninverted resonances. To verify the proposed spin diffusion pathway the experiment of Fig. 2c is carried out with a triply modulated pulse. Figure 2d shows the offset profile recorded for $E64 H^N$ in ubiquitin, using two-way cross-polarization (18). Thus we isolate the three-spin system $E64 H^N$, $F4 H^\epsilon$, and $E64 H^\alpha$ allowing spin diffusion within this subnetwork while suppressing to zero order the transfer to and from the environment. The spin diffusion pathway which was previously suppressed is now reactivated, as evidenced by the reappearance of the signal due to $F4 H^\epsilon$.

Figure 3 shows a detail taken from the X-ray structure (19) of ubiquitin. Protons were added using the program Sybyl (Rohm and Haas Company). Displayed are the spin diffusion pathways alluded to in Fig. 2. One may observe that $E64 H^\alpha$ is located between $E64 H^N$ and $F4 H^\epsilon$ accounting for the observed two-step transfer. Conversely a one-step transfer seems more likely in the case of $S65 H^N$.

Figure 4 shows buildup curves for the targets $S65 H^N$ and $F4 H^\epsilon$. The curves have been normalized with respect to the source peak extrapolated back to zero mixing time. In the fitting procedure we first determine the 4×4 relaxation matrix from the unquenched experimental data. One then calculates an average Liouvillian composed of $\Gamma^{(0)}$ and $\Gamma^{(1)}$ to describe the case where $E64 H^\alpha$ is inverted. Relaxation during the selective pulse has been neglected. The resulting curves are in good agreement with signal amplitudes observed in the quenched experiments. $S65 H^N$ remains substantially unchanged suggesting that the NOE is not mediated by $E64 H^\alpha$. Conversely the buildup for $F4 H^\epsilon$ shows a large attenuation when spin diffusion is suppressed. Although the curves give an improved evaluation of the cross-relaxation rates, caution should be taken as only selected diffusion pathways have been eliminated. There will in general be many pathways that mediate the flow of magnetization.

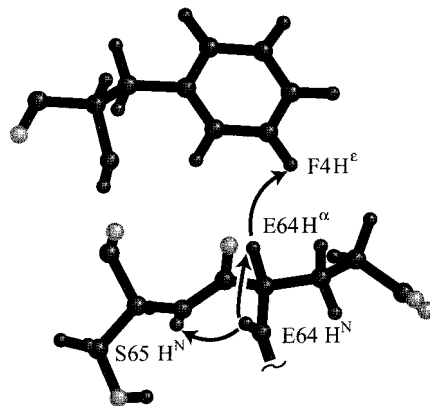


FIG. 3. Detail from the X-ray structure of ubiquitin in the vicinity of the source proton $E64 H^N$. Highlighted are the transfer steps corresponding to the buildup curves of Fig. 4.

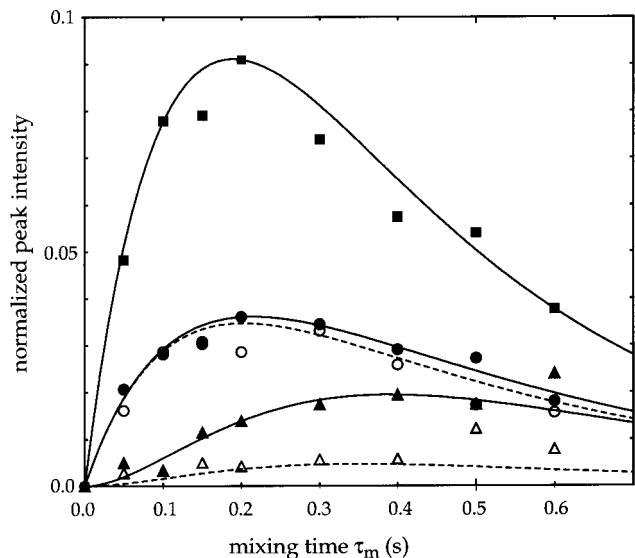


FIG. 4. Normalized buildup curves for target protons E64 H $^\alpha$ (■), S65 H N (●), and F4 H $^\alpha$ (▲). Filled symbols and solid lines correspond to normal NOE measurements, as in Fig. 2a. A 4×4 matrix was fitted to the filled symbols using an initial matrix calculated from the X-ray distances assuming a rigid molecule in isotropic motion. This matrix is then used to calculate an average Liouvillian for the case where E64 H $^\alpha$ is inverted at $\tau_m/2$ as in Fig. 2b (open symbols and dashed lines).

The use of average Liouvillian theory has been shown to yield a more physical interpretation of spin diffusion effects. In particular imperfect suppression is readily described by invoking a first-order correction without need to resort to an exact solution of the Solomon equations.

ACKNOWLEDGMENTS

This work was supported by the Fonds National de la Recherche Scientifique, by the Commission pour la Technologie et l'Innovation of Switzerland, and by the Centre National de la Recherche Scientifique of France.

REFERENCES

1. J. Cavanagh, W. J. Fairbrother, A. G. Palmer III, and N. J. Skelton, "Protein NMR Spectroscopy: Principles and Practice," Academic Press, New York (1996).
2. W. Massefski Jr. and A. G. Redfield, Elimination of multiple-step spin diffusion effects in two-dimensional NOE spectroscopy of nucleic acids, *J. Magn. Reson.* **78**, 150–155 (1988).
3. S. Macura, J. Fejzo, C. G. Hoogstraten, W. M. Westler, and J. L. Markley, Topological editing of cross-relaxation networks, *Isr. J. Chem.* **32**, 245–256 (1992).
4. C. G. Hoogstraten, W. M. Westler, S. Macura, and J. L. Markley, Improved measurement of longer proton–proton distances in proteins by relaxation network editing, *J. Magn. Reson. B* **102**, 232–235 (1993).
5. C. Zwahlen, S. J. F. Vincent, L. Di Bari, M. H. Levitt, and G. Bodenhausen, Quenching spin diffusion in selective measurements of transient Overhauser effects in nuclear magnetic resonance. Applications to oligonucleotides, *J. Am. Chem. Soc.* **116**, 362–368 (1994).
6. Z. Zolnai, N. Juranic, J. L. Markley, and S. Macura, Magnetization exchange network editing: Mathematical principles and experimental demonstration, *Chem. Phys.* **200**, 161–179 (1995).
7. S. J. F. Vincent, C. Zwahlen, and G. Bodenhausen, Suppression of spin diffusion in selected frequency bands of nuclear Overhauser spectra, *J. Biomol. NMR* **7**, 169 (1996).
8. S. J. F. Vincent, C. Zwahlen, C. B. Post, J. W. Burgner, and G. Bodenhausen, The conformation of NAD $^+$ bound to lactate dehydrogenase determined by nuclear magnetic resonance with suppression of spin diffusion, *Proc. Natl. Acad. Sci. USA* **94**, 4383 (1997).
9. C. G. Hoogstraten and A. Pardi, Improved distance analysis in RNA using network-editing techniques for overcoming errors due to spin diffusion, *J. Biomol. NMR* **11**, 85 (1998).
10. N. Juranic, Z. Zolnai, and S. Macura, Identification of spin diffusion pathways in proteins by isotope-assisted NMR cross-relaxation network editing, *J. Biomol. NMR* **9**, 317–322 (1997).
11. E. Chiarparin, P. Pelupessy, B. Cutting, T. R. Eykyn, and G. Bodenhausen, Normalized one-dimensional NOE measurements in isotopically labeled macromolecules using two-way cross-polarization, *J. Biomol. NMR* **13**, 61–65 (1999).
12. M. H. Levitt and L. Di Bari, Steady state in magnetic resonance pulse experiments, *Phys. Rev. Lett.* **69**, 3124–3127 (1992).
13. M. H. Levitt and L. Di Bari, The homogeneous master equation and the manipulation of relaxation networks, *Bull. Magn. Reson.* **16**, 94–114 (1994).
14. R. Ghose, T. R. Eykyn, and G. Bodenhausen, Average Liouvillian theory revisited: Cross correlated relaxation between chemical shift anisotropy and dipolar couplings in the rotating frame in nuclear magnetic resonance, *Mol. Phys.*, in press (1999).
15. M. Schwager and G. Bodenhausen, Quantitative determination of cross-relaxation rates in NMR using selective pulses to inhibit spin diffusion, *J. Magn. Reson. B* **111**, 40–49 (1996).
16. D. Marion, M. Ikura, and A. Bax, Improved solvent suppression in one- and two-dimensional NMR spectra by convolution of time-domain data, *J. Magn. Reson.* **84**, 425–430 (1989).
17. H. Geen and R. Freeman, Band-selective radiofrequency pulses, *J. Magn. Reson.* **93**, 93–141 (1991).
18. T. R. Eykyn, R. Ghose, and G. Bodenhausen, Offset profiles of selective pulses in isotopically labeled macromolecules, *J. Magn. Reson.* **136**, 211–213 (1999).
19. S. Vijay-Kumar, C. E. Bugg, and W. J. Cook, Structure of ubiquitin refined at 1.8 Å resolution, *J. Mol. Biol.* **194**, 531–544 (1987).